RASĀYAN *J. Chem.*
Vol. 18 | No. 4 |1906-1912| October-December | 2025
ISSN: 0974-1496 | e-ISSN: 0976-0083 | CODEN: RJCABP
http://www.rasayanjournal.com
http://www.rasayanjournal.co.in

PREPARATION, CHARACTERIZATION, AND MAGNETIC PROPERTY STUDY OF SILICA-COATED IRON OXIDE NANOPARTICLES

K. Satyam Naidu[1,2,✉], Nowduri Annapurna[2], R. S. K. Sharma[1], G. V. Siva Prasad[1], M. Ravi kumar[1] and V. Anita[1]

[1]Department of Chemistry, Raghu Engineering College (A), Visakhapatnam-531162, (AP), India
[2]Department of Engineering Chemistry, AUCE(A), (AU), Visakhapatnam-530003, (AP), India
✉Corresponding author: satymnaidu.kandi@raghuenggcollege.in

ABSTRACT

Magnetic nanoparticles (MNPs), particularly SiO_2@Fe_3O_4 core-shell structures, are promising in biomedical applications like magnetic hyperthermia therapy (MHT) due to their biocompatibility and efficient heat generation under alternating magnetic fields (AMF). In this study, Fe_3O_4 and SiO_2@Fe_3O_4 MNPs were synthesized via reverse co-precipitation and a modified Stöber method. Structural and morphological analyses were conducted using XRD, FTIR, SEM, TEM, and XPS, while VSM assessed magnetic behavior. Particle sizes were approximately 6 nm (Fe_3O_4) and 8 nm (SiO_2@Fe_3O_4). Magnetic studies confirmed superparamagnetic behavior, indicating their potential for MHT. This work aligns with SDG 3: Good Health and Well-being, by contributing to the advancement of non-invasive therapeutic approaches for non-communicable diseases such as cancer.

Keywords: Magnetic Nanoparticles, Silica-Coated Fe_3O_4 Stober Process, Magnetic Hyperthermia, Super Magnetism.
RASAYAN *J. Chem.*, Vol. 18. No. 4, 2025

INTRODUCTION

Magnetic nanoparticles (MNPs) with well-controlled properties have attracted considerable attention in the biomedical field, specifically aimed at medical diagnostics and treatment due to their nanoscale size and unique magnetic behaviors.[1,2] Among these, Fe_3O_4 (magnetite) and γ-Fe_2O_3 (maghemite) are the most widely studied, offering super Para magnetism and low toxicity, making them ideal for uses such as MRI[1], cell sorting, enzyme immobilization[1], biosensing and bio-electrocatalysis[1], nucleic acid purification[3,4,] tumor therapy[5], and targeted drug delivery.[6,7] Extensive research has focused on various synthesis and characterization techniques to produce high-performance Fe_3O_4 MNPs.[8] Ideal MNPs require chemical stability, uniform size distribution, and good dispersibility. To prevent oxidation and preserve magnetic behavior, a protective coating is essential. Amphoteric hydroxyl ions (H_3O^+/OH^-) aid stability via electrostatic repulsion and interaction with counterions.[9,10] Recent advances focus on silica-coated Fe_3O_4 MNPs.[11] Iron oxide's strong affinity for silica enables straightforward amorphous silica coating via sol–gel methods.[12] Silica encapsulation improves chemical stability and enables Nano device self-assembly for bio molecular uses.[13,14,15] This self-assembly, central to supramolecular chemistry[16], relies on non-covalent forces such as H-bonding, metal coordination, and van der Waals interactions, offering additional oxidative protection.[17] Silica surfaces form silanol (Si–OH) groups, which readily react with organosilanes through Si–O–Si covalent bonds. Surfactant-induced Langmuir monolayers exemplify this process.[18,19,20] providing a stable interface for biomolecule interaction. Amorphous silica has gained prominence as a coating material in the past decade.[21,22,23] The strength and structural performance of magnetic nanocomposites depend greatly on the uniformity and level of magnetic phase dispersion in the SiO_2 framework. Small, single-domain nanoparticles are preferred for their high magnetization under external fields. Silica encapsulation prevents oxidation, minimizes iron ion leakage, and provides a biocompatible surface for biomolecular interactions.[24] Its hydrophilicity further facilitates purification procedures.[25,26] As a result, silica-coated magnetic beads are increasingly employed in biomedical fields cell separation, drug delivery, tumor cell removal, and genetic analysis through nucleic acid (DNA/RNA) extraction.[27,28] Magnetic separation techniques also enable efficient protein purification due to their phase-switching capability and

http://doi.org/10.31788/RJC.2025.1849389
This work is licensed under a CC BY 4.0 license.

high surface area. Additionally, they are useful in pathogen detection and diagnostics.[29] SiO_2@Fe_3O_4 MNPs are particularly promising in magnetic hyperthermia therapy (MHT) due to their biocompatibility and efficient heat induction under an alternating magnetic field (AMF). The Fe_3O_4 core ensures superparamagnetic response, while the SiO_2 shell enhances colloidal stability, prevents aggregation, and supports functionalization for targeted drug delivery.[30,31] Optimized particle sizes (~10–50 nm) and controlled coatings improve dispersion and reduce cytotoxicity. These MNPs can selectively elevate tumor temperatures to 42–45 °C, promoting apoptosis and enhancing chemo/radiotherapy. Current research targets improved surface engineering, combinational therapies, and in vivo efficacy and safety.[32,33] This study focuses on the synthesis of Fe_3O_4 MNPs and their silica-coated counterparts, examining their structural and magnetic properties. FTIR analysis assessed chemical composition, while XRD confirmed crystal structure. XPS provided element-specific structural insights, and TEM evaluated crystal morphology and silica coating quality. This work aligns with SDG-3: Good Health and Well-being, by contributing to the advancement of non-invasive therapeutic approaches for non-communicable diseases such as cancer.

EXPERIMENTAL

Materials

All substances involved in the preparation of Fe_3O_4 and SiO_2@Fe_3O_4 were of analytical reagent (AR) grade and did not require any further refining. Ferrous Sulphate heptahydrate [$FeSO_4 \cdot 7H_2O$] (98%), ammonium hydroxide [NH_4OH] (25%), tetraethyl orthosilicate (TEOS), and ethanol were all supplied by Sigma Aldrich and were used as received.

Synthesis of SiO_2@Fe_3O_4 Composite NPs

The SiO_2@Fe_3O_4 (MNPs) were synthesized using a reverse co-precipitation process (Scheme-1). Initially, 100 mL of a 0.05M ferrous Sulphate heptahydrate solution,20 mL of 98% ethanol, was mixed with 1 mL of TEOS and stirred for 120 minutes. Then, 7 mL of 25% ammonium hydroxide was added to this mixture, which was stirred further for 15 minutes. Following this, the hydrolysis and condensation of TEOS were performed under continuous stirring for 12 hours. pH is adjusted to 13 during the procedure. Finally, the product was rinsed with ethanol, then dried in a furnace at 600°C before being pulverized into a fine powder.

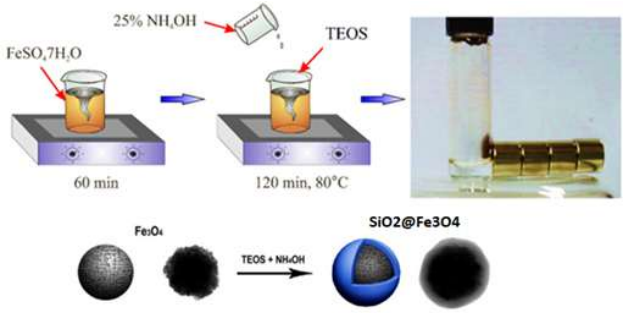

Scheme-1: Graphical abstract of SiO_2@ Fe_3O_4 MNP

Experimental Setup for Studying Magnetic Properties

A Vibrating Sample Magnetometer was utilized to evaluate the magnetic behavior of the samples. In this technique, the sample is vibrated within a uniform magnetic field, which induces a changing magnetic flux. According to Faraday's Law, the fluctuation in magnetic flux produces a voltage in the sensing coils, directly related to the magnetization of the material. The VSM records the magnetic hysteresis loop, which provides important parameters such as coercivity, saturation magnetization, and remanence, offering valuable insights into the sample's ferromagnetic behavior.

RESULTS AND DISCUSSION

X-Ray Diffraction (XRD) Study

Figure-1 confirms the crystalline structure of both Fe_3O_4 and SiO_2@Fe_3O_4 NPs. The characteristic peaks matched those in the JCPDS card no. 19-0639, with the most intense peak appearing at 35.87°, which corresponds to the γ-Fe_3O_4 phase. After coating with SiO_2, the patterns showed signals from both magnetite

and silica, but the Fe_3O_4 crystal structure remained largely unaffected. A slight broadening of peaks suggested the particles were nanoscale in size, estimated at about 6 nm for Fe_3O_4 and around 8 nm for $SiO_2@Fe_3O_4$. These findings are in good agreement with previously reported studies.

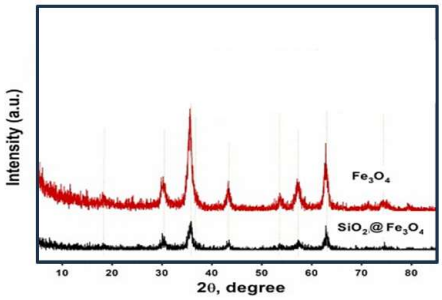

Fig.-1: XRD Pattern of Prepared $SiO_2@ Fe_3O_4$

FTIR Spectroscopy Study

Figure-2 displays the FTIR spectra of Fe_3O_4 and $SiO_2@Fe_3O_4$ nanoparticles. The characteristic Fe–O–Fe stretching vibration at 640 cm^{-1} confirmed the presence of Fe_3O_4. A distinct band at 1400 cm^{-1} indicated Fe–O–Si bonding, which confirms that the SiO_2 coating was successful. Additionally, peaks observed at 1102 cm^{-1} and 790 cm^{-1} corresponded to the stretching and bending vibrations of the O–Si–O group, further verifying the presence of silica.

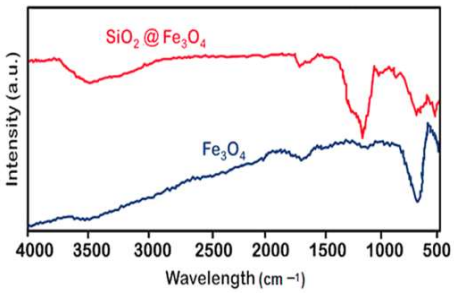

Fig.-2: FTIR image of Prepared $SiO_2@ Fe_3O_4$

X-ray Photoelectron Spectroscopy (XPS) Study

Figure-3 displays the XPS survey spectra of Fe_3O_4 nanoparticles and their silica-coated counterparts. The presence of iron, oxygen, and silicon was confirmed by photoelectron peaks at approximately 710/725 eV (Fe 2p), 533 eV (O 1s), and 106 eV (Si 2p), respectively. Notably, the intensity of the Fe peaks was reduced in the $SiO_2@Fe_3O_4$ sample, indicating that the Fe_3O_4 core was successfully encapsulated by the silica shell.

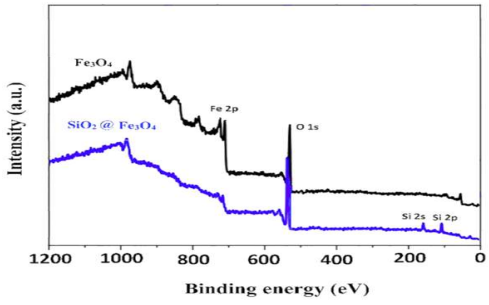

Fig.-3: XPS Survey Spectrum of $SiO_2@ Fe_3O_4$

Scanning Electron Microscopy (SEM) Study

Figure-4 displays SEM images, which demonstrate that the $SiO_2@Fe_3O_4$ nanoparticles are mostly well dispersed, although small agglomerates are still present due to residual magnetic and van der Waals forces between the magnetite cores. While silica coating improves colloidal stability, it does not entirely prevent clustering. The slight variations in particle size across the sample likely reflect differences in nucleation and growth rates during synthesis.

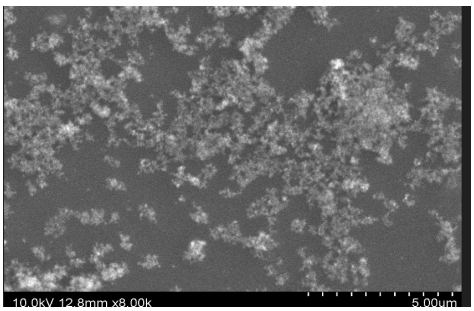

Fig.-4: SEM images of the Surface of SiO_2@ Fe_3O_4

Transmission Electron Microscopy (TEM) Study

TEM analysis (Fig.-5a & 5b) showed that Fe_3O_4 nanoparticles have a spherical shape with some size variation. For the SiO_2@Fe_3O_4 nanoparticles, clear core-shell structures were observed, consisting of a magnetite core around 6 nm in size, the structure is encased in a silica shell measuring about 2 nm in thickness. This confirms successful coating and consistent nanoscale size. Figure-5c presents the particle size distribution in the form of a histogram, indicating that the particles range in size from 4 to 14 nm, exhibiting an average size close to 8 nm. Further, the SAED (Fig.-5d) patterns typically display concentric discrete spots corresponding to the spinel cubic structure of magnetite, with reflections indexed to planes such as (220), (311), (400), and (511).

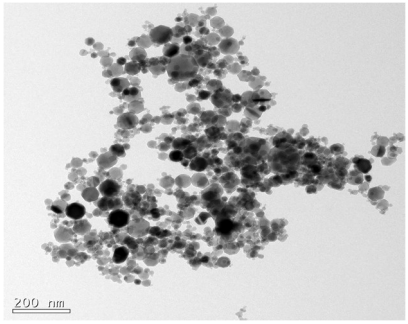

Fig.-5: (a) TEM image of the SiO_2@ Fe_3O_4

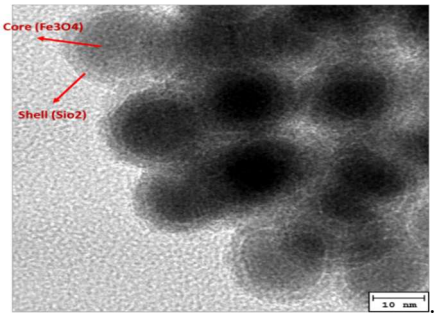

Fig.-5: (b) TEM image of SiO_2@Fe_3O_4 NP

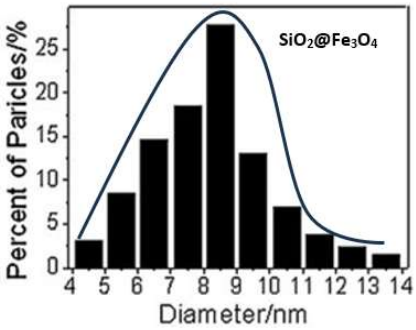

Fig.-5: (c) Size Distribution of SiO_2@Fe_3O_4 NP.

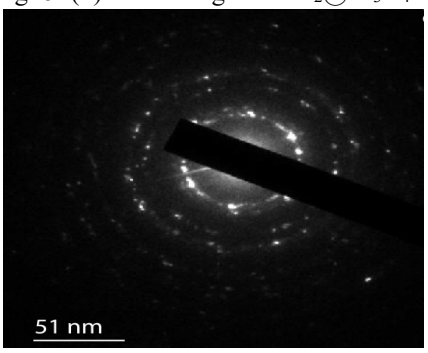

Fig.-5: (d) SAED of SiO_2@Fe_3O_4 NP.

Magnetic(M-H) Study

Figure-6 and Table-1 illustrate the magnetic behavior of Fe_3O_4 and SiO_2@Fe_3O_4 NPs. The measured saturation magnetization (Ms) values were found to be 83.5 and 42.3 emu/g, respectively, demonstrating ferromagnetic behaviour at room temperature. The lower Ms value in the SiO_2@Fe_3O_4 sample is attributed to the dilution effect caused by the non-magnetic silica shell. Both samples showed superparamagnetic characteristics, supported by their low remanence and coercivity. This is typical for nanoparticles smaller than 10 nm, consistent with the ~8 nm size determined by XRD. These magnetic properties suggest that these materials could be well-suited for applications such as magnetic hyperthermia.

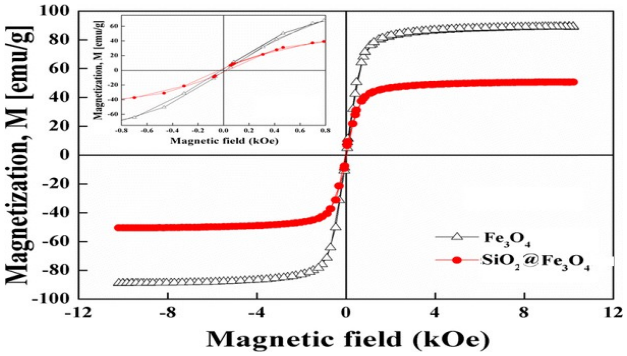

Fig.-6: Magnetic Hysteresis Loop of SiO_2@ Fe_3O_4

Table-1: Characterization of Magnetic Properties in the Synthesized MNPs

S. No.	Sample(s)	Saturation Magnetization [Ms] (emu g^{-1})	Remanent Magnetization [Mr] (emu g^{-1})	Coercivity [Hc] (Koe)
1	Fe_3O_4 MNp	83.5	0.137	3.42
2	$SiO_{2@}Fe_3O_4$ MNp	42.3	0.119	1.49

CONCLUSION

SiO_2@Fe_3O_4 magnetic nanoparticles were successfully prepared via a reverse coprecipitation process. Structural analyses confirmed crystalline magnetite cores with uniform silica shells. The Si–O–Fe interface influenced magnetic behavior by introducing antiferromagnetic interactions and reducing ferromagnetic coupling. Magnetic studies revealed superparamagnetic properties with low remanence and coercivity, ideal for applications like magnetic hyperthermia and targeted drug delivery. The silica coating enhanced stability, biocompatibility, and surface functionalization potential. Future research should focus on surface modification, biocompatibility evaluation, and optimizing in vivo performance for advanced biomedical applications.

ACKNOWLEDGMENTS

The authors gratefully acknowledge Raghu Engineering College and the Department of Engineering Chemistry, Andhra University, for their support and facilities. Special thanks to the REC Chemistry Department Head and colleagues for their technical assistance and guidance.

CONFLICT OF INTERESTS

The authors declare that there is no conflict of interest.

AUTHOR CONTRIBUTIONS

The present work is related to *SDG-3: Good Health and Well-being*. All the authors contributed significantly to this manuscript, participated in reviewing/editing and approved the final draft for publication. The research profile of the authors can be verified from their ORCID ids, given below:

K. Satyam Naidu https://orcid.org/0000-0003-4985-9206
Nowduri Annapurna https://orcid.org/0000-0003-4946-5362
G. V. Siva Prasad https://orcid.org/0009-0004-8693-4185
R. S. K. Sharma https://orcid.org/0000-0001-9338-8208
M. Ravi Kumar https://orcid.org/0009-0004-9040-198X
V. Anita https://orcid.org/0009-0007-6509-6022

Open Access: This article is distributed under the terms of the Creative Commons Attribution 4.0 International License (http://creativecommons.org/licenses/by/4.0/), which permits unrestricted use, distribution, and reproduction in any medium, provided you give appropriate credit to the original author(s) and the source, provide a link to the Creative Commons license, and indicate if changes were made.

REFERENCES

1. H. Fatima, K. S. Kim, *Advanced Powder Technology: International Journal of the Society of Powder Technology,* **29(11)**, 2678(2018), https://doi.org/10.1016/j.apt.2018.07.017.

2. S. Ni, X. Sun, X. Wang, G. Zhou, F. Yang, J. Wang, D. He, *Materials Chemistry and Physics*, **124(1),** 353(2010), https://doi.org/10.1016/j.matchemphys.2010.06.046.
3. Z. W. Li, Z. H. Yang, *Journal of Magnetism and Magnetic Materials*, **387**, 131(2015), https://doi.org/10.1016/j.jmmm.2015.03.087
4. K. E. McCloskey, J. J. Chalmers, M. Zborowski, *Analytical Chemistry*, **75(24),** 6868(2003), https://doi.org/10.1021/ac034315j
5. H.-Y. Park, M. J. Schadt, L. Wang, I.-I. S. Lim, P. N. Njoki, S. H. Kim, C.-J. Zhong, *Langmuir: The ACS Journal of Surfaces and Colloids*, **23(17),** 9050(2007), https://doi.org/10.1021/la701305f
6. S. Gao, Y. Shi, S. Zhang, K. Jiang, S. Yang, Z. Li, E. Takayama-Muromachi, *The Journal of Physical Chemistry C: Nanomaterials and Interfaces*, **112(28),** 10398(2008), https://doi.org/10.1021/jp802500a
7. J. Santoyo-Salazar, M. A. Castellanos-Roman, L. B. Gómez, *Materials Science & Engineering C: Materials for Biological Applications*, **27(5)**, 1317(2007), https://doi.org/10.1016/j.msec.2006.07.027
8. P. S. Haddad, T. M. Martins, L. D'Souza-Li, L. M. Li, K. Metze, R. L. Adam, D. Zanchet, *Materials Science & Engineering C: Materials for Biological Applications*, **28(4)**, 489(2008), https://doi.org/10.1016/j.msec.2007.04.014
9. K. Park, G. Liang, X. Ji, Z.-P. Luo, C. Li, M. C. Croft, J. T. Markert, *The Journal of Physical Chemistry C: Nanomaterials and Interfaces*, **111(50),** 18512(2007), https://doi.org/10.1021/jp0757457
10. M. Bonini, A. Wiedenmann, P. Baglioni, *Materials Science and Engineering C*, **26(5**), 745(2006), https://doi.org/10.1016/j.msec.2005.09.042
11. M. Stjerndahl, M. Andersson, H. E. Hall, D. M. Pajerowski, M. W. Meisel, R. S. Duran, *Langmuir*, **24(7**), 3532(2008), https://doi.org/10.1021/la7035604
12. M. E. Khosroshahi, L. Ghazanfari, *Physica E: Low-Dimensional Systems and Nanostructures*, **42(6),** 1824(2010), https://doi.org/10.1016/j.physe.2010.01.042
13. Y. Kobayashi, S. Saeki, M. Yoshida, D. Nagao, M. Konno, *Journal of Sol-Gel Science and Technology*, **45(1),** 35(2008), https://doi.org/10.1007/s10971-007-1648-1
14. D. Yang, J. Hu, S. Fu, *Journal of Physical Chemistry C*, **113(18),** 7646(2009), https://doi.org/10.1021/jp900868d
15. A. Ali, H. Zafar, M. Zia, I. Ul Haq, A. R. Phull, J. S. Ali, A. Hussain, *Nanotechnology, Science and Applications*, **9**, 49(2016), https://doi.org/10.2147/NSA.S99986
16. T. Yang, C. Shen, Z. Li, H. Zhang, C. Xiao, S. Chen, H. Gao, *Journal of Physical Chemistry B*, **109(49),** 23233(2005), https://doi.org/10.1021/jp054291f
17. M. I. Khalil, *Arabian Journal of Chemistry*, **8(2),** 279(2015), https://doi.org/10.1016/j.arabjc.2015.02.008
18. T. Ahn, J. H. Kim, H.-M. Yang, J. W. Lee, J.-D. Kim, *Journal of Physical Chemistry C*, **116(10),** 6069(2012), https://doi.org/10.1021/jp211843g
19. X. Zhang, W. Wu, J. Wang, X. Tian, *Applied Surface Science*, **254(9),** 2893(2008), https://doi.org/10.1016/j.apsusc.2007.10.022
20. M. Arroyo-Hernández, R. J. Martín-Palma, J. Pérez-Rigueiro, J. P. García-Ruiz, J. L. García-Fierro, J. M. Martínez-Duart, *Materials Science and Engineering C*, **23(6),** 697(2003), https://doi.org/10.1016/j.msec.2003.09.159
21. H. Cao, J. He, L. Deng, X. Gao, *Applied Surface Science*, **255(18),** 7974(2009), https://doi.org/10.1016/j.apsusc.2009.04.199
22. S.-J. Lee, J.-R. Jeong, S.-C. Shin, J.-C. Kim, J.-D. Kim, *Journal of Magnetism and Magnetic Materials*, **282**, 147(2004), https://doi.org/10.1016/j.jmmm.2004.04.035
23. M. Mahdavi, M. B. Ahmad, M. J. Haron, F. Namvar, B. Nadi, M. Z. A. Rahman, J. Amin, *Molecules*, **18(7),** 7533(2013), https://doi.org/10.3390/molecules18077533
24. J.-R. Jeong, S.-J. Lee, J.-D. Kim, S.-C. Shin, *Physica Status Solidi B*, **241(7),** 1593(2004), https://doi.org/10.1002/pssb.200304549
25. M. Gonzales-Weimuller, M. Zeisberger, K. M. Krishnan, *Journal of Magnetism and Magnetic Materials*, **321(13),** 1947(2009), https://doi.org/10.1016/j.jmmm.2008.12.017
26. W. Wu, Q. He, C. Jiang, *Nanoscale Research Letters*, **3(11),** 397(2008), https://doi.org/10.1007/s11671-008-9174-9

27. T. Hyeon, S. S. Lee, J. Park, Y. Chung, H. B. Na, *Journal of the American Chemical Society*, **123(51),** 12798(2001), https://doi.org/10.1021/ja016812s
28. S. Sun, H. Zeng, *Journal of the American Chemical Society*, **124(28),** 8204(2002), https://doi.org/10.1021/ja026501x
29. K. Woo, J. Hong, S. Choi, H.-W. Lee, J.-P. Ahn, C. S. Kim, S. W. Lee, *Chemistry of Materials*, **16(14),** 2814(2004), https://doi.org/10.1021/cm049552x
30. J. Park, E. Lee, N.-M. Hwang, M. Kang, S. C. Kim, Y. Hwang, T. Hyeon, *Angewandte Chemie International Edition*, **44(19),** 2873(2005), https://doi.org/10.1002/anie.200461665
31. S. Santra, R. Tapec, N. Theodoropoulou, J. Dobson, A. Hebard, W. Tan, *Langmuir*, **17(10**), 2900(2001), https://doi.org/10.1021/la0008636
32. A. B. Chin, I. I. Yaacob, *Journal of Materials Processing Technology*, **191(1),** 235(2007), https://doi.org/10.1016/j.jmatprotec.2007.03.011
33. X.-D. Che, H. N. Bertram, *Journal of Magnetism and Magnetic Materials*, **116(1),** 121(1992), https://doi.org/10.1016/0304-8853(92)90155-h

[RJC-9389/2025]